Characterization and Analysis on the Solder Ball Shear Testing Conditions

Xingjia Huang[1], S.-W. Ricky Lee[1,2], Chien Chun Yan[2], and Sam Hui[3]

[1]/ Department of Mechanical Engineering
[2]/ Electronic Packaging Laboratory
Hong Kong University of Science & Technology
Clear Water Bay, Kowloon, Hong Kong

[3]/ Department of Electrical Engineering
Stanford University
Stanford, CA, USA

Abstract

This paper presents both experimental investigation and computational analysis on the solder ball shear testing conditions for ball grid array (BGA) packages. The experimental data of solder ball shear tests indicate that the ram height and the shear speed have substantial effects on the solder ball shear strength. The general trend shows that lower ram height and faster shear speed can result in higher ball shear strength. A two-dimensional finite element model is established to simulate the solder ball shear tests. The results in terms of load-displacement curve from computational analysis are in good agreement with the experimental data. Based on the computational stress analysis, an effort is made to interpret the failure mode of solder balls subject to the ball shear test.

Introduction

Ball grid array (BGA) and flip chip (FC) technologies are the main themes for IC packaging industries in the 90s. The BGA and FC packages have many advantages over conventional modules. Among them are larger I/O, lower profile, smaller form factors, and better thermal/electrical performance [1-3]. Furthermore, these advanced packages are compatible with the surface mount technology (SMT), consequently, leading to high throughput and low assembly cost for mass production. For surface mounted components (SMCs), the solder joints are not only the passage of electrical signals, power, and ground, but also the mechanical support to hold the module in position on the printed circuit board (PCB). Therefore, the solder joint reliability is a major concern for BGA and FC packages.

Currently the most popular method to evaluate the strength of solder ball attachment is the ball shear test. The typical value of solder ball shear force may range from 30 g_f (for 4-mil FC solder bumps) to more than 1000 g_f (for 30-mil BGA solder balls) [1, 4-12]. Although such tests are simple and convenient to implement, there is not much mechanics justification to interpret the testing results. Most people still use the method of A-to-B comparison to determine the acceptance of packages. The conventional ball shear test method [7, 8, 12-15] is adopted from the gold ball shear test of wire bonding [16]. In July of 2000, JEDEC established a new standard, JESD22-B117, for BGA ball shear tests [17]. In this publication, only the ram height is standardized. The specification is that the gap between the edge of the shear ram and the surface of ball mounting should be larger than 0.05 mm (2 mils) and smaller than (or equal to) 25% of the ball height. However, another important testing parameter, the shear speed (loading rate), is not addressed in this standard. The lack of specification in shear speed sometimes may cause confusion in the comparison of solder ball shear strengths characterized with very different loading rates. It should be noted that in most cases the fracture surface cuts through the solder during the ball shear test. To interpret the failure mechanism needs not only the materials knowledge but also the detailed mechanics explanation. Therefore, further research efforts for understanding the rationale of solder ball shear tests and interpreting the failure mechanism are still in great demand.

The present study is aimed at establishing the mechanics foundation for the ball shear tests to evaluate the solder ball attachment strength of the BGA packages. In particular, the emphases are placed on the investigation of testing conditions such as ram height and shear speed and on the understanding of failure mechanism. In this paper, both experimental investigation and computational modeling are presented. Specimens with BGA solder balls are fabricated and ball shear tests with various testing conditions are conducted. Computational stress analyses are performed with an established finite element model to interpret the failure mechanism.

Experimental Procedures

The objective of the present study is to investigate the effect of various ram heights and shear speed on the shear strength of solder balls. The specimens under evaluation were standard 0.76 mm (30 mils) 63Sn-37Pb spheres for PBGA applications. The substrates for solder ball attachment were BT laminates with a thickness of 0.46 mm. The solder bond pads were solder-mask-defined with an opening of 0.6 mm in diameter. The metallization of bond pads was Cu with Ni/Au electro-plating. The solder balls were attached to the bond pads using standard SMT reflow profile. After the reflow, the average ball height and diameter were 0.64 mm and 0.78 mm, respectively. Figure 1 shows the cross-section of a solder ball.

The ball shear tests were conducted using a Dage 4000S machine. The ball shear testing conditions are given in Tables 1 and 2. For each testing condition, 25 solder balls were sheared. During each run, the displacement and the corresponding shear force were recorded.

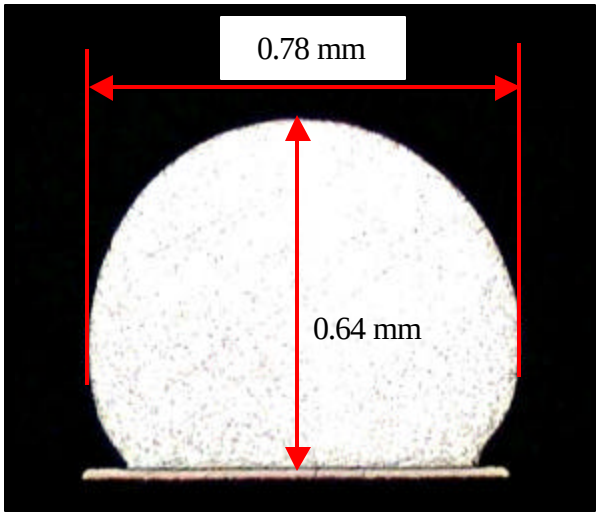

Figure 1: Cross-section of Solder Ball

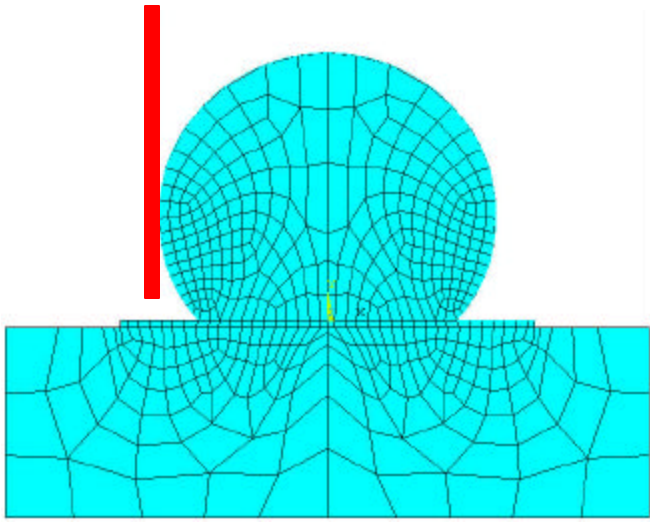

Figure 2: Finite Element Model for Ball Shear Test

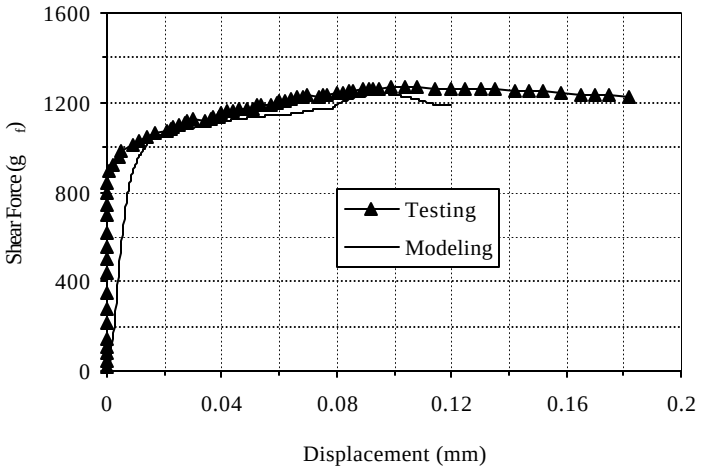

Figure 3: Force-Displacement Curves of Base Case (Height: 10%, Speed: 100 µm/s)

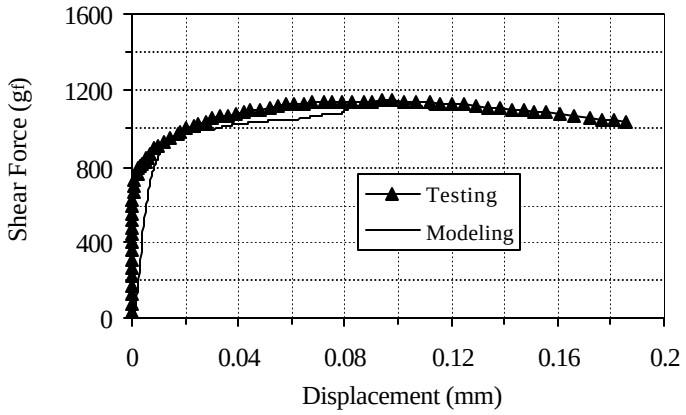

(a) Speed: 20 µm/s

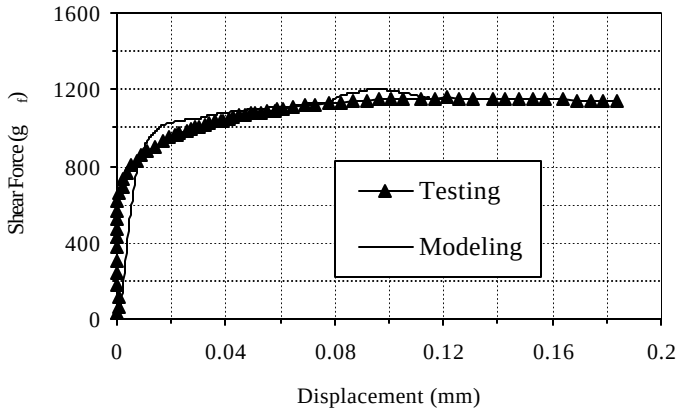

(b) Speed: 50 µm/s

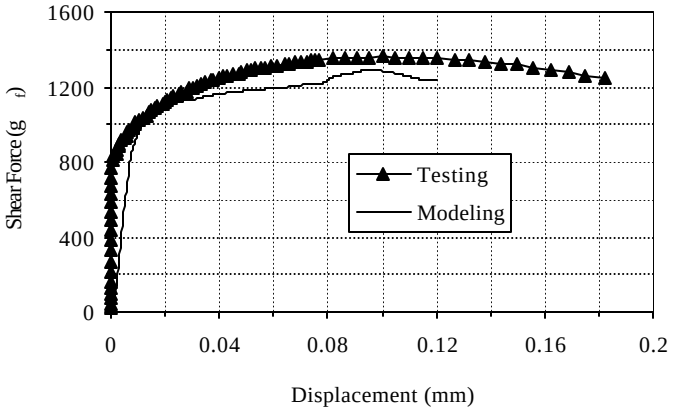

(c) Speed: 200 µm/s

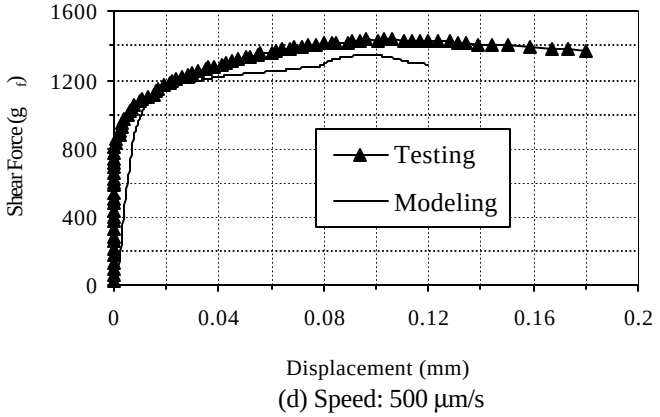

(d) Speed: 500 µm/s

Figure 4: Force-Displacement Curves with Various Shear Speeds (Fixed Height: 10%)

Table 1: Ball Shear Tests with Fixed Ram Height and Various Shear Speeds

Height (μm)	Shear Speed (μm/s)				
64 (10%)	20	50	100	200	500

Note: (* %) – percentage of the ball height.

Table 2: Ball Shear Tests with Fixed Shear Speed and Various Ram Heights

Speed (μm/s)	Ram Height (μm)				
100	32 (5%)	64 (10%)	128 (20%)	160 (25%)	192 (30%)

Note: (* %) – percentage of the ball height.

Finite Element Analysis (FEA)

In the present study, a 2-D computational model with dimensions measured from the cross-section was established as shown in Figure 2 to simulate the solder ball shear test. A commercial finite element code, ANSYS v.5.6, was used. The solder ball, the bond pad, and the substrate were modeled by 8-node plane strain elements (PLANE183). The shear ram was considered as a rigid body. A feature in ANSYS using the surface-to-surface target element (TARGE169) and the contact element (CONTA172) was employed to simulate the contact behavior between the shear ram and the solder ball. Since this was a time-dependent non-linear analysis, both large deformation and transient options were enabled.

In the finite element model, except the solder ball, all other constituents were considered as linear-elastic materials. The elastic material properties used in modeling are listed in Table 3.

Table 3: Elastic Material Properties for Modeling

Materials	E (MPa)	ν	ρ (g/cm^3)
63Sn-37Pb	29,800	0.40	8.41
Cu pad	128,700	0.34	8.31
BT Substrate	14,000	0.39	1.2

In the present analysis, the eutectic solder was treated as a material with elastic-viscoplastic response. The creep behavior is governed by the equation given below [18]:

$$\frac{d\varepsilon_c}{dt} = C_1[\sinh(C_2\sigma)]^{C_3}\exp\left(-\frac{C_4}{T}\right) \qquad (1)$$

The constitutive relation in Eq. (1) is an existing option in ANSYS v.5.6 and can be easily implemented using the parameters listed in Table 4.

Table 4: Creep Option Input Parameters for ANSYS v.5.6

C_1 (sec^{-1})	C_2	C_3 (MPa^{-1})	C_4 (°K)
339.0102	3.3	0.062653	6,360

Results of Ball Shear Strength and Comparison

In the present study, the shear test condition with the ram height of 64 μm and the shear speed of 100 μm/s was chosen as the base case. The effect of changing the ram height and shear speed on the shear strength of solder balls was investigated.

Figure 3 shows the results of shear force-displacement curve under the testing conditions of base case. The data of other cases with a fixed ram height and various shear speeds are presented in Figure 4. In all cases, the testing and modeling results are in good agreement. Comparing Figure 3 with Figure 4, one can find that, with the increase of shear speed, the shear force-displacement curve moves upwards. This indicates that faster shear speed results in higher shear force. It should be noted that, for each curve, there exists a peak load, which is considered the shear strength of tested solder ball. More detailed analyses on the FEA results reveal that the peak load usually corresponds to the displacement when the tip of the shear ram just begins to cut into the solder ball. Afterwards the shear force starts to descend.

Figure 5 presents the results of shear force-displacement curves for the solder ball shear tests with a fixed shear speed and various ram heights. It can be seen that, with the increase of ram height, the shear force-displacement curve moves downwards, indicating the decrease of ball shear strength. It should be noted that, for the cases shown in Figures 5 (c) and 5(d), the curves given by FEA terminate earlier than those of other cases. This is because the local deformation in the solder has become too severe (the edge of ram cuts deep into the solder ball due to large ram height). In the aforementioned figures, it seems that the curves are leveling off. However, the numerical values indicate all curves (both testing and modeling) have started to descend. Therefore, it is still feasible to find the peak loads. Note that the ram heights in the last two cases are 25% and 30% of the ball height, respectively. The former is right on the margin and the latter has gone beyond the margin specified in JESD22-B117. Relatively large deviations in the peak loads between testing and modeling are observed for these two cases.

The finite element model established in the present study was two-dimensional. The original shear force values obtained from the ANSYS were in force per unit thickness (e.g. N/mm). To obtain the actual shear forces, all the original force data must be multiplied by a scale factor (effective thickness). Unfortunately, there is no formula available to calculate such effective thickness. However, since the fracture surface of ball shear tests is very close to the bond pad and the pad opening diameter is 0.6 mm, it is obvious that the effective thickness of the 2-D model must be smaller than 0.6 mm. With such observation, the scale factor of effective thickness can be estimated in the following manner.

For the base case (10% ram height, 100 μm/s shear speed), the direct reading of peak shear force from ANSYS was 2969 g_f/mm. Compared with the corresponding value from testing (1244 g_f), the effective thickness was determined as 0.42 mm. Subsequently, this value was applied to all other cases. From Figures 4 and 5, it is clear that the same effective thickness yields to good agreement between testing and modeling for all cases. Therefore, it can be concluded that the selected effective thickness was not a random coincidence. It should carry a certain physical meaning, which represents the scale factor between the 2-D and 3-D analysis. Furthermore, the fact that the chosen effective thickness is smaller than 0.6 mm enhances the confidence in the previous selection.

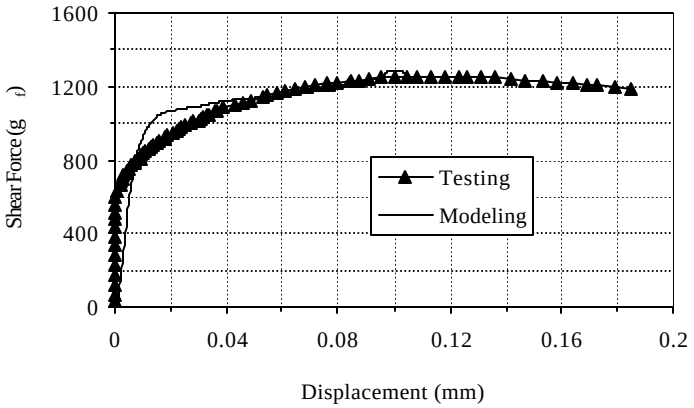

(a) Height: 5%

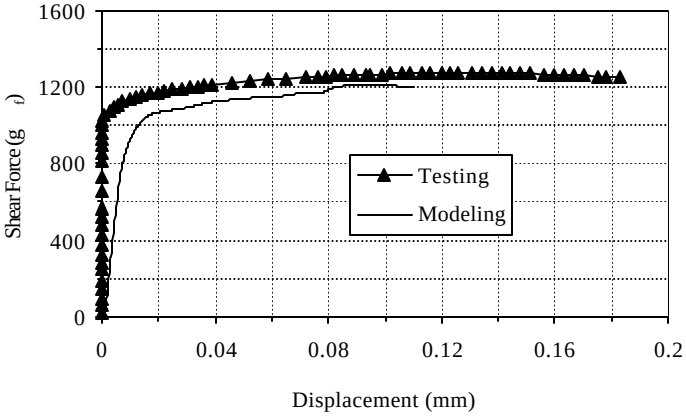

(b) Height: 20%

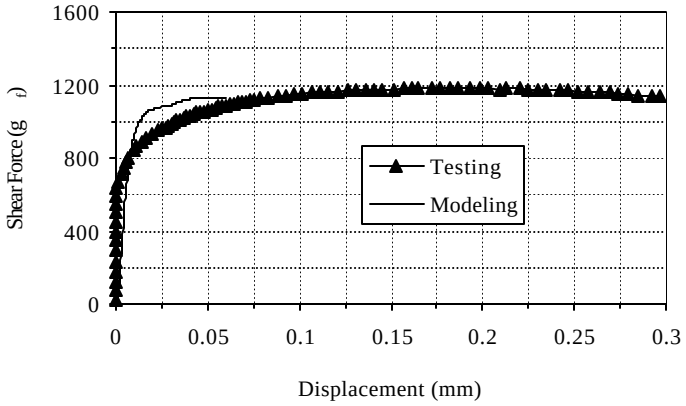

(c) Height: 25%

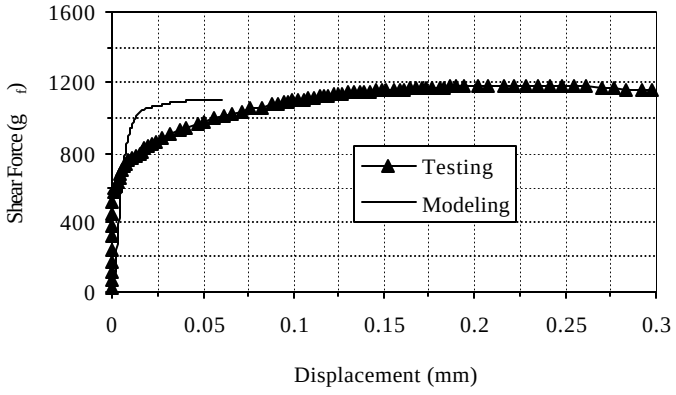

(d) Height: 30%

Figure 5: Force-Displacement Curves with Various Ram Heights (Fixed Speed: 100 µm/s)

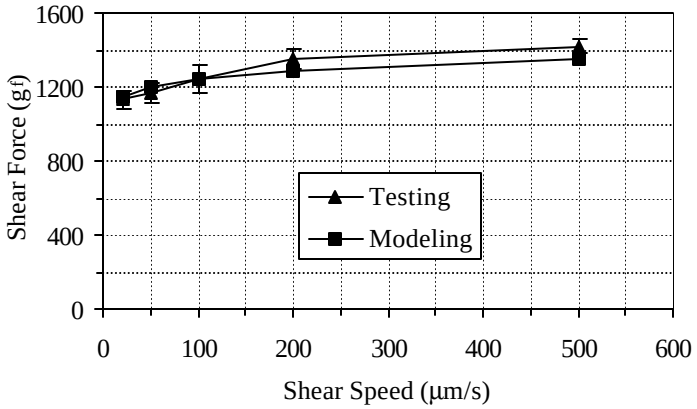

Figure 6: Effect of Shear Speed on Ball Shear Strength

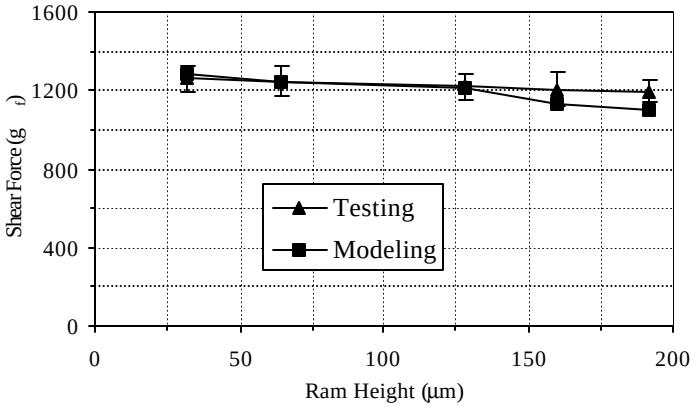

Figure 7: Effect of Ram Height on Ball Shear Strength

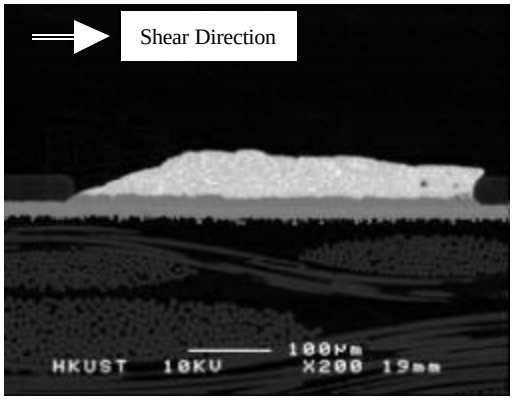

Figure 8: Typical Cross-section after Ball Shear Test

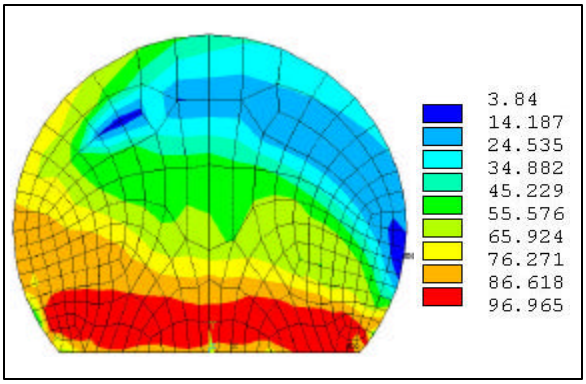

Figure 9: von Mises Stress Contours of Base Case

It should be noted that, for all curves shown in Figures 3-5, the peak values of shear force are regarded as the shear strength of solder balls. The ball shear strengths from testing and modeling with fixed ram height and fixed shear speed are listed in Tables 5 and 6, respectively. For the ease of comparison, the data in these two tables are plotted in Figures 6 and 7. The trend shows that the ball shear strength increases for either faster shear speed or lower ram height. Another point to be noted is that, although in general the shear strengths from testing and modeling are in good agreement, there are relatively big discrepancies for the cases with ram height larger than 20% or shear speed faster than 100 μm/s. From this point of view, we may deduce that the ideal solder ball shear testing conditions are the cases with ram height smaller than 25% and shear speed slower than 200 μm/s.

Table 5: Ball Shear Strength with Fixed Ram Height

Ram Height (64 μm)	Shear Speed (μm/s)				
	20	50	100	200	500
Testing	1131 (46)	1171 (54)	1244 (77)	1350 (53)	1418 (38)
Modeling	1143	1202	1247	1291	1350

Note: (*) – Standard Deviation, Unit – g_f.

Table 6: Ball Shear Strength with Fixed Shear Speed

Shear Speed (100 μm/s)	Ram Height (μm)				
	32	64	128	160	192
Testing	1259 (68)	1244 (77)	1219 (68)	1207 (83)	1193 (56)
Modeling	1282	1247	1208	1131	1104

Note: (*) – Standard Deviation, Unit – g_f.

Discussion on Failure Mode

From the experimental results, it is known for ball shear tests that most failures occur close to the bond pad surface but in the bulk of solder material [7, 8, 12, 13]. Figure 8 is a typical cross-section micrograph after the ball shear test [12], showing clearly the failure mode.

Figure 9 shows the contours of von Mises stress distribution in the solder ball at the peak load for the base case ball shear test. The shear ram moves from the left to the right. From the comparison between Figure 8 and Figure 9, it is observed that the ball shear failure mode is closely related to the high stress region of von Mises stress contours. More stress contour plots with various testing conditions are given in Figure 10. In general, except for the extreme case of large ram height (30%), the stress contour pattern does not vary too much. However, the stress level does change among various cases, giving different ball shear strengths.

Figure 11 presents the contours of von Mises creep strain distribution (corresponding to the stress contours shown in Figure 10) in the solder ball. The general trends are more or less the same as those observed from the stress contours. It should be noted that the present failure mode matching is a very primitive approach. For more sophisticated analyses, extra efforts will be required to consider the crack propagation after the initial failure and the resulting path of fracture surface.

Summary and Conclusions

In the present study, both experimental investigation and computational modeling were performed to study the effects of ram height and shear speed on the solder ball shear strength. The results are summarized as follows.

- The ram height and shear speed have substantial effects on the solder ball shear strength. The data from both testing and modeling indicated that lower ram height and faster shear speed would result in higher ball shear strength.
- The results from testing and modeling were in good agreement. An effective thickness was identified for the 2-D plane strain analysis. With such a scale factor, it is feasible to study 3-D problems with a 2-D model.
- The ideal solder ball shear test conditions were recommended to be the cases with ram height smaller than 25% and shear speed slower than 200 μm/s.
- The failure mode of ball shear tests seemed to match with the von Mises stress/strain contour pattern in the solder ball.

Although the present analyses were performed for the solder balls of BGA package, the methodology may be applied to other cases such as the solder bumps of flip chip. With the assistance of computational stress analyses, meaningful comparisons among different packages may be achieved. The results obtained from this study should be very helpful for the electronics manufacturing industry to interpret their testing data and determine the acceptance criteria for the products with solder ball attachment.

References

1. J. H. Lau and Y. H. Pao, *Solder Joint Reliability of BGA, CSP, Flip Chip, and Fine Pitch SMT Assemblies*, McGraw-Hill, NY, 1997.
2. J. H. Lau, *Low Cost Flip Chip Technologies*, McGraw-Hill, NY, 2000.
3. J. H. Lau, *Flip Chip Technologies*, McGraw-Hill, NY, 1996.
4. M. Klein, B. Wiens, M. Hutter, H. Oppermann, R. Aschenbrenner, H. Reichl, "Behaviour of Platinum as UBM in Flip Chip Solder Joints," *Proc. 50th ECTC*, May 21-24, 2000, Nevada, pp. 40-45.
5. R. H. Uang, K. C. Chen, S. W. Lu, H. T. Hu and S. H. Huang, "The Reliability Performance of Low Cost Bumping on Aluminum and Copper Wafer," *Proc. 3rd Electronics Packaging Technology Conference (EPTC 2000)*, December 5-7, 2000, Singapore, pp. 292-296.
6. J. M. Jao, T. D. Her, C. P. Huang, E. Ho. G. Calub, R. H. Y. Lo, "Study of a New Structured Leadframe Based CSP, mini-LOC," *Proc. 50th ECTC*, May 21-24, 2000, Nevada, pp. 364-369.
7. C. H. Zhong, S. Yi, Y. C. Mui, C. P. Howe, D. Olsen and W. T. Chen, "Missing Solder Ball Failure Mechanisms in Plastic Ball Grid Array Packages," *Proc. 50th ECTC*, May 21-24, 2000, Nevada, pp. 151-159.

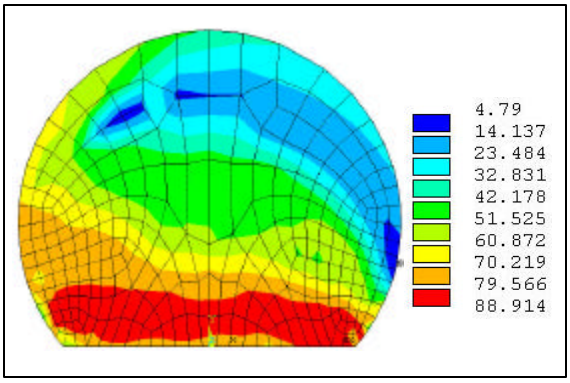

(a) Height: 10%, Speed: 20 μm/s

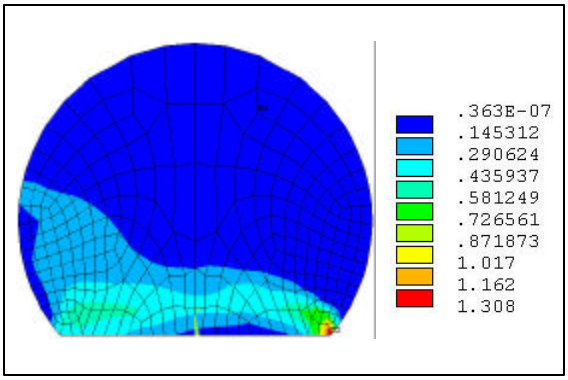

(a) Height: 10%, Speed: 20 μm/s

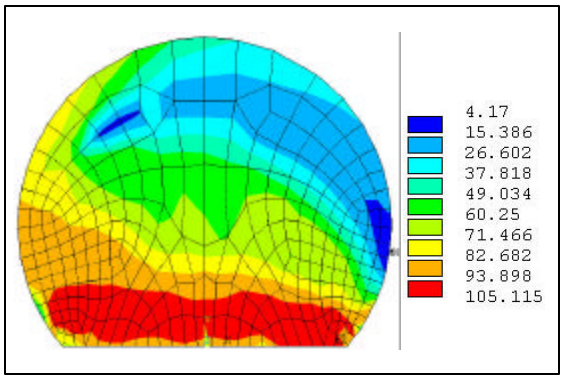

(b) Height: 10%, Speed: 500 μm/s

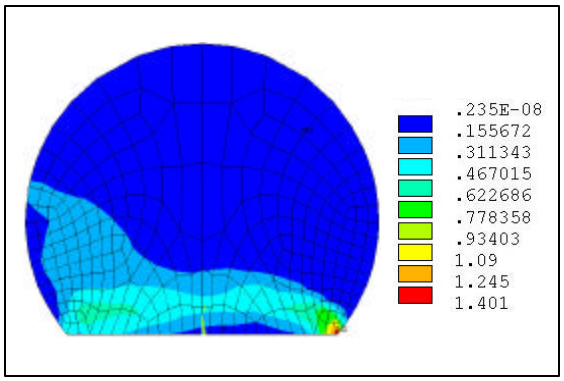

(b) Height: 10%, Speed: 500 μm/s

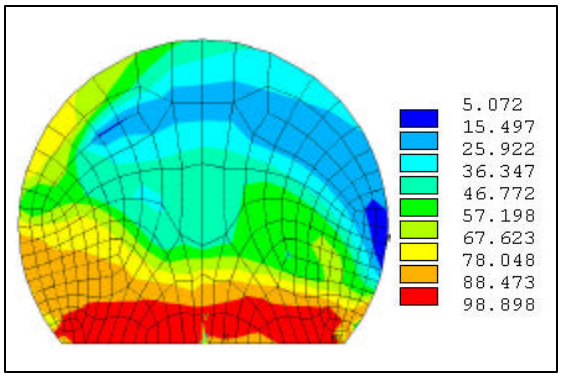

(c) Height: 5%, Speed: 100 μm/s

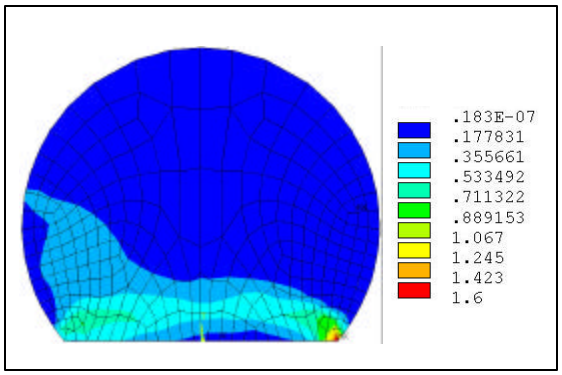

(c) Height: 5%, Speed: 100 μm/s

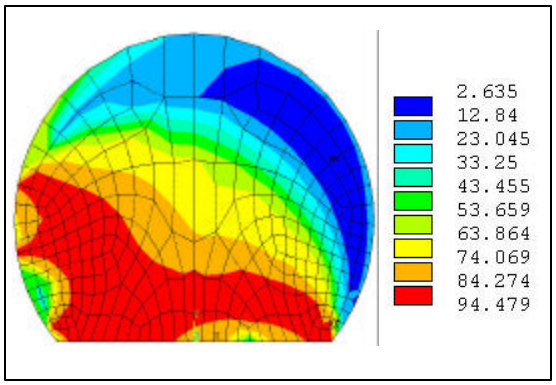

(d) Height: 30%, Speed: 100 μm/s

Figure 10: Comparison of von Mises Stress Contours

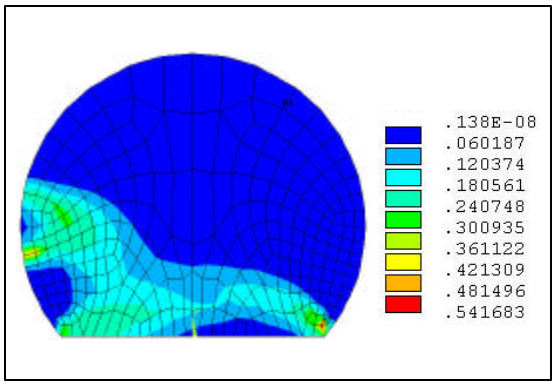

(d) Height: 30%, Speed: 100 μm/s

Figure 11: Comparison of Inelastic Strain Contours

8. R. J. Coyle, P. P. Solan, A. J. Serafino and S. A. Gahr, "The Influence of Room Temperature Aging on Ball Shear Strength and Microstructure of Area Array Solder Balls," *Proc. 50th ECTC*, May 21-24, 2000, Nevada, pp. 160-169.
9. K. M. Levis and A. Mawer, "Assembly and Solder Joint Reliability of Plastic Ball Grid Array with Lead-free versus Lead-Tin Interconnect," *Proc. 50th ECTC*, May 21-24, 2000, Nevada, pp. 1198-1204.
10. Y. Tomita, Q. Wu, A. Maeda, S. Baba and N. Ueda, "Advanced Surface Plating on the Organic FC-BGA Package," *Proc. 50th ECTC*, May 21-24, 2000, Nevada, pp. 861-867.
11. I. S. Kang, J. H. Kim, I. S. Park, K. R. Hur, S. J. Cho, H. Han and J. Yu, "The Solder Joint and Runner Metal Reliability of Wafer-Level CSP (Omega-CSP)," *Proc. 50th ECTC*, May 21-24, 2000, Nevada, pp. 87-92.
12. S.-W. R. Lee, C. C. Yan, Z. Karim and X. Huang, "Assessment on the Effect of Electroless Nickel Plating on the Reliability of Solder Ball Attachment to the Bond Pads of PBGA Substrate," *Proc. 50th ECTC*, May 21-24, 2000, Nevada, pp. 868-873.
13. C. K. Shin and J. Y. Huh, "Effect of Cu-containing Solders on the Critical IMC Thickness for the Shear Strength of BGA Solder Joints," *Proc. 3rd Electronics Packaging Technology Conference (EPTC2000)*, December 5-7, 2000, Singapore, pp. 406-411.
14. S. Y. Jang and K. W. Paik, "Comparison of Electroplated Eutectic Sn/Bi and Pb/Sn Solder Bumps on Various UBM Systems," *Proc. 50th ECTC*, May 21-24, 2000, Nevada, pp. 64-68.
15. S. J. Cho, J. Y. Kim, M. G. Park, I. S. Park and H. S. Chun, "Under Bump Metallurgies for a Wafer Level CSP with Eutectic Pb-Sn Solder Ball," *Proc. 50th ECTC*, May 21-24, 2000, Nevada, pp. 844-849.
16. ASTM F1269-89 "Test Methods for Destructive Shear Testing of Ball Bonds," *1991 Annual Book of ASTM Standards*, Vol. 10.04, 1991, ASTM, Philadelphia.
17. JESD22-B117 "BGA Ball Shear," July 2000, JEDEC Solid State Technology Association.
18. S.-W. R. Lee, K. Newman and L. Hu, "Thermal Fatigue Analysis of PBGA Solder Joints with the Consideration of Damage Evolution," *Packaging of Electronic and Photonic Devices*, EEP-Vol. 28, November 5-10, Florida, 2000, pp. 207-212.